Progress in Neurobiology 256 (2026) 102856

Contents lists available at ScienceDirect

Progress in Neurobiology

journal homepage: www.elsevier.com/locate/pneurobio

Glycine and glycine transport control dendritic excitability and spiking

Kirsten Bohmbach [a,1], Vincent Bauer [a,1], Christian Henneberger [a,b,*,2]

[a] Institute of Cellular Neurosciences I, Medical Faculty, University of Bonn, Germany
[b] German Center for Neurodegenerative Diseases (DZNE), Bonn, Germany

ARTICLE INFO

Keywords:
Glycine
Glycine transport
N-methyl-D-aspartate receptors
Dendritic excitability
Dendritic spiking
D-serine
Hippocampus

SUMMARY

Neuronal dendrites integrate excitatory input. They can perform local computations such as coincidence detection by amplifying synchronized local input and dendritic spiking. Extracellular glycine could be a powerful modulator of such processes through its action as a co-agonist at glutamate receptors of the N-methyl-D-aspartate (NMDA) subtype but also as a ligand of inhibitory glycine receptors (GlyRs). Similarly, glycine transporters (GlyTs), an emerging drug target for psychiatric and other diseases, could control dendritic integration through ambient glycine levels. Both hypotheses were tested at dendrites of CA1 pyramidal cells in acute hippocampal slices by pharmacologically analysing how glycine, GlyTs and GlyRs change the postsynaptic response to local dendritic excitatory input. Using microiontophoretic glutamate application, we found that glycine can indeed significantly increase dendritic excitability and dendritic spiking. We also uncovered that GlyTs are powerful modulators of dendritic spiking, which can limit the impact of glycine sources on CA1 pyramidal cells. Our experiments also revealed that GlyRs can have an opposite, inhibitory effect on the slow dendritic spike component. This directly demonstrates that glycine can dynamically enhance dendritic responsiveness to local input and promote dendritic spiking, while GlyTs and GlyRs have an opposing effect. Together, this makes glycinergic signalling a powerful modulator of the nonlinear integration of synaptic input in CA1 radial oblique dendrites.

1. Introduction

Neuronal dendrites receive and integrate excitatory synaptic input. They can also amplify the depolarization caused by simultaneously active local synapses through voltage-dependent mechanisms. Voltage-dependent sodium channels and glutamate receptors of the N-methyl-D-aspartate subtype (NMDARs) can contribute to this amplification and the resulting dendritic spikes in CA1 pyramidal cell dendrites (Ariav et al., 2003; Losonczy and Magee, 2006; Stuart and Spruston, 2015; Bohmbach et al., 2022). Such dendritic spiking is thought to be important, for example, for coincidence detection, synaptic plasticity and the representation and formation of place fields in the hippocampus (Remy and Spruston, 2007; Sheffield et al., 2017; Poirazi and Papoutsi, 2020).

Since NMDARs can participate in the amplification of synaptic input, the regulation of their activity shapes dendritic spiking. An important regulatory site on the NMDAR is the co-agonist binding site, which needs to be bound with either glycine or D-serine for the NMDAR receptors to open (Johnson and Ascher, 1987; Kleckner and Dingledine, 1988). Because the level of occupancy of the NMDAR co-agonist binding site can vary in an activity-dependent manner (Bergeron et al., 1998; Tsai et al., 2004; Henneberger et al., 2010; Papouin et al., 2017; Robin et al., 2018; Adamsky et al., 2018; Koh et al., 2022), we recently investigated if changing levels of extracellular D-serine modify dendritic spiking. Indeed, we observed that activity-dependent D-serine release facilitates dendritic spiking through an astrocytic mechanism, which tunes spatial memory formation (Bohmbach et al., 2022). In contrast, it is currently not known to our knowledge if the NMDAR co-agonist glycine plays a similar or different role.

Differences are expected compared to D-serine, because extracellular glycine has different signalling targets and its extracellular concentration is controlled by different mechanisms. Apart from conventional NMDARs and their co-agonist binding site, glycine can also directly act on hippocampal inhibitory glycine receptors (GlyRs) (Sipila et al., 2004; Zhang et al., 2008a; Xu and Gong, 2010) and a subpopulation of excitatory GluN3A-containing NMDARs (Bossi et al., 2023; Hurley et al., 2024). In addition, it is mainly glycine transporters (GlyTs) that control

* Corresponding author at: Institute of Cellular Neurosciences I, Medical Faculty, University of Bonn, Germany.
E-mail address: christian.henneberger@uni-bonn.de (C. Henneberger).
[1] K.B. and V.B. contributed equally to this study.
[2] Lead contact

https://doi.org/10.1016/j.pneurobio.2025.102856
Received 3 July 2025; Received in revised form 19 November 2025; Accepted 21 November 2025
Available online 24 November 2025

the levels of extracellular glycine (Bergeron et al., 1998; Martina et al., 2004; Tsai et al., 2004; Xu and Gong, 2010) and that mediate activity-dependent glycine release near CA1 pyramidal cell dendrites (Zhang et al., 2018). GlyTs have also emerged as an important drug target for the treatment cognitive deficits in disease that are thought to involve NMDAR hypofunction like schizophrenia (Lane et al., 2010; Möhler et al., 2011; Nakazawa and Sapkota, 2020; Fleischhacker et al., 2021; Rosenbrock et al., 2023) and potentially also stroke (Cappelli et al., 2022). For these reasons, we have explored how glycine and GlyTs control the dendritic response to local glutamatergic input and dendritic spiking via NMDARs and GlyRs.

2. Results

2.1. Glycine modulates dendritic spiking

First, we examined how exogenous glycine affects dendritic responses to increasing local excitatory input using iontophoretic glutamate application during whole-cell patch clamp recordings from CA1 pyramidal cells (Fig. 1**a-c**). We have previously confirmed that NMDARs contribute significantly to dendritic spiking in this experimental setting and that experimental results are qualitatively equivalent to alternative techniques for probing dendritic spiking like two-photon glutamate uncaging on sets of dendritic spines (Bohmbach et al., 2022). The evoked dendritic spikes recorded at the soma have a characteristic time course directly related to local dendritic mechanisms (Losonczy and Magee, 2006; Bohmbach et al., 2022). After the initial slow start of the excitatory postsynaptic potential (EPSP), the activation of voltage-dependent conductances (e.g. voltage-gated sodium channels) leads to an all-or-nothing dendritic spike which is detectable as a fast component in the postsynaptic potential and its first derivative (dV/dt; Fig. 1c, asterisk). This is followed by a slower component, to which NMDAR activity contributes significantly (Losonczy and Magee, 2006; Harnett et al., 2012; Bohmbach et al., 2022). We emulated a stepwise increase of local excitatory input by increasing the amount of iontophoretically applied glutamate (Fig. 1**c**). Dendritic spiking was identified by the appearance of a fast component in the postsynaptic response (Fig. 1**c**, right panels, asterisk) and characterized by determining the threshold stimulus (i.e. the lowest amount of iontophoretically applied glutamate eliciting a dendritic spike, Fig. 1**c**, vertical dashed orange line), the amplitude of the slow component (Fig. 1**c,** black arrow), and the amplitude of the largest subthreshold response (Fig. 1**c**, green data point). Dendritic responses throughout the manuscript were characterized by these parameters as illustrated in Fig. 1**c**. To isolate the action of glycine via NMDARs we performed these recordings in the presence of the GlyR inhibitor strychnine. After obtaining a baseline recording, 100 μM glycine was bath-applied (Fig. 1**d**). This concentration was chosen because it reliably saturates the NMDAR co-agonist binding site of the relevant NMDAR isoforms in expression systems (Matsui et al., 1995; Chen et al., 2008) without causing internalization of NMDARs (Chen et al., 2003; Cappelli et al., 2022). It was also chosen because it is above the EC50 of GlyRs (Lozovaya et al., 2005) of CA1 pyramidal cells,

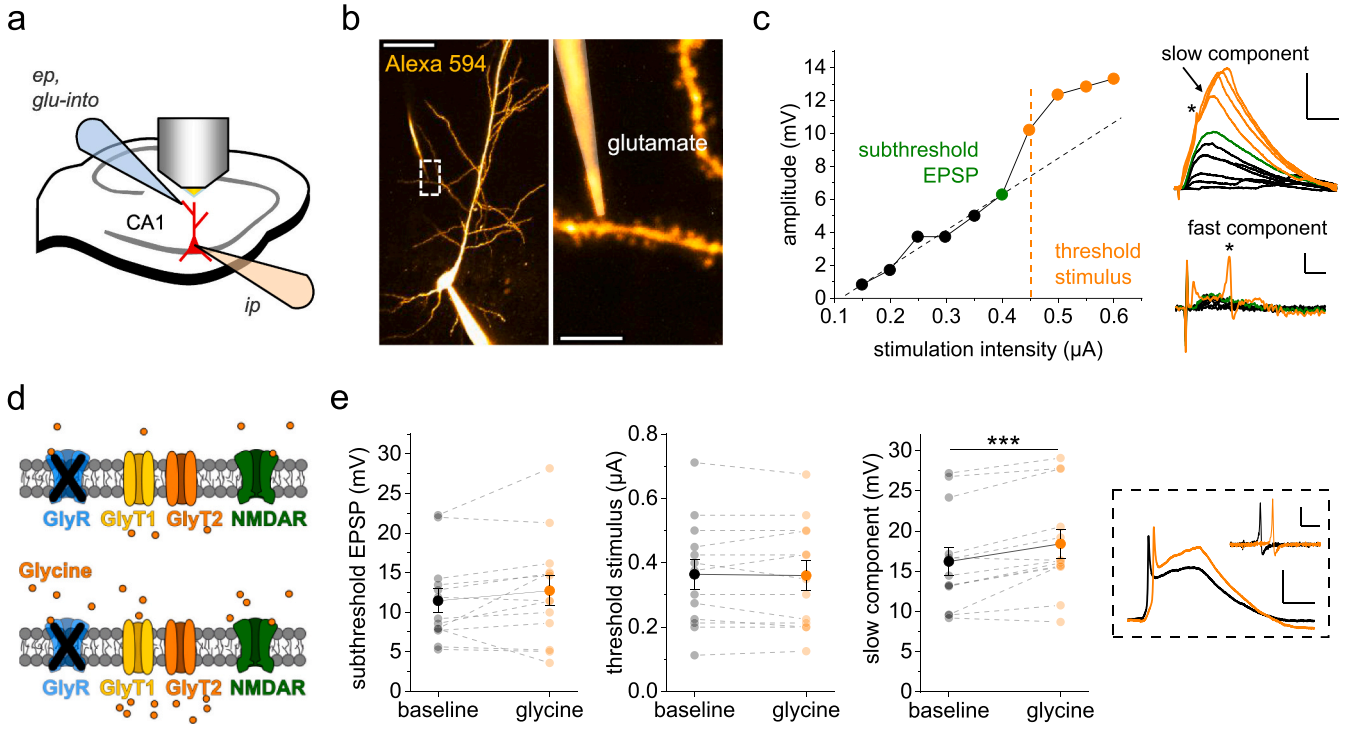

Fig. 1. Probing glycinergic control of dendritic spiking in CA1 pyramidal cells. a) Schematic of acute slice experiments. Whole-cell patch clamp recordings (ip, intracellular orange pipette, current clamp), iontophoretic glutamate application (ep, extracellular blue pipette), two-photon excitation (2PE) imaging of patched neuron and iontophoresis pipette filled with Alexa Fluor 594 (40 μM and 50 μM, respectively). **b)** Example image (left panel: scale bar 50 μm; right panel: zoom in on dashed box in left panel, scale bar 5 μm). **c)** Example relationship between glutamate application and somatically recorded response. Data points in left panel: black below dendritic spike threshold, green for last subthreshold EPSP and orange for dendritic spikes. Vertical orange line indicates the threshold stimulus for evoking a dendritic spike. Right panels: corresponding sample traces. Upper right panel: scale bars 5 mV and 20 ms. Lower right panel: dV/dt for identification of the fast spike component (asterisk), scale bars 1 mV/ms and 5 ms. **d)** Schematic experimental protocol for **e**: Acute application of glycine with blocked glycine receptors (GlyR, blue) and intact glycine transporters (GlyT1 and GlyT2, yellow and orange). Upper panel: baseline. Lower panel: acute glycine bath application (100 μM, orange dots). **e)** Glycine did not change the subthreshold EPSP amplitudes (left panel, 11.45 ± 1.53 mV vs. 12.72 ± 1.90 mV, n = 13, z = -1.68, p = 0.094, two-sided Wilcoxon Signed Ranks test), the threshold stimulus (middle panel, 0.36 ± 0.05 μA vs. 0.36 ± 0.05 μA, n = 13, t(12) = 0.44, p = 0.67, two-sided paired Student's t test) but increased the slow component of dendritic spikes (right panel, 16.22 ± 1.73 mV vs. 18.42 ± 1.76 mV, n = 13, t(12) = -4.60, p = 0.00061, two-sided paired Student's t test). Dashed box: sample traces of dendritic spikes recorded during baseline (black) and after application of glycine (orange, scale bars: 5 mV and 20 ms, inset: 10 mV/ms and 5 ms). Data are expressed and displayed as mean ± s.e.m.

whose contribution to dendritic spiking was analysed in later experiments. Under these experimental conditions (GlyRs inhibited), acute glycine application led to an isolated increase of the slow dendritic spike component without a change of the dendritic spike threshold or subthreshold response (Fig. 1**e**). In control recordings without glycine application, theses parameters (i.e. subthreshold EPSP, threshold stimulus, slow component) were stable (Supplementary table 1). This is qualitatively different from the effect of the NMDAR co-agonist D-serine, which, as reported previously (Bohmbach et al., 2022), lowers the required excitatory drive for generating a dendritic spike (i.e. decreases the threshold) and increases the slow component. Because glycine and D-serine at the used concentrations should both be saturating the NMDAR co-agonist binding site, these results suggest that either glycine is not reaching the NMDARs at the nominal concentration, or that the co-agonists have different effects through the NMDARs.

Therefore, we next asked if D-serine has an additional effect on dendritic spiking in the presence of bath-applied glycine (illustrated in Fig. 2**a**). As before, glycine alone only increased the slow component amplitude of dendritic spikes, but D-serine in addition to glycine lowered the threshold stimulus and increased the slow component and the subthreshold EPSP amplitude (Fig. 2**b**). The cumulative effect of D-serine and glycine on the slow component of ~ 25 % (Fig. 2**c**) is near identical to the one of D-serine alone (23 %) (Bohmbach et al., 2022), which is consistent with the idea that glycine and D-serine are affecting dendritic spiking through the same NMDAR population and mechanisms.

2.1.1. *Glycine transporters limit glycine effects on dendritic spiking*

These results suggest that exogenous glycine does not reach NDMARs at the nominal concentration, because 100 μM glycine should have saturated to NMDAR co-agonist binding site thereby preventing additional effects of D-serine. Indeed, it is well established that glycine transporters represent a powerful uptake mechanisms that controls NMDAR activity (Chen et al., 2003; Martina et al., 2004; Supplisson, 2024) and thus could prevent applied glycine from fully reaching NMDARs. To test this hypothesis, we probed dendritic spiking and its sensitivity to NDMAR co-agonists in the presence of both the glycine transporter 1 (GlyT1) antagonists NFPS (5 μM) and the glycine transporter 2 (GlyT2) antagonist Org 25543 (1 μM) (referred to as GlyT1/2 blockade or inhibition). In a first experiment, acute blockade of GlyT1/2 selectively increased the slow dendritic spike component (Fig. 3**a-b**), which is in line with an increase of extracellular glycine concentration after GlyT1/2 inhibition (Zhang et al., 2018) and similar to application of glycine alone (Fig. 1**e**). We next tested how GlyT1/2 inhibition changes the effect of glycine on dendritic spiking by first applying glycine and GlyT1/2 inhibitors together and then in combination with D-serine (Fig. 3**c**). Under these conditions, glycine reduced the threshold stimulus, increased the subthreshold EPSP and the slow spike component, and D-serine had no further effect on these parameters of dendritic spiking (Fig. 3**d-e**). This demonstrates that the effects of glycine on dendritic integration are strongly limited by GlyT1/2 activity at resting conditions. It also emphasizes that, under these conditions, glycine and D-serine act through the same NMDAR population because glycine occludes the effect of additional D-serine.

While the expression and functional relevance of GlyT1 in the

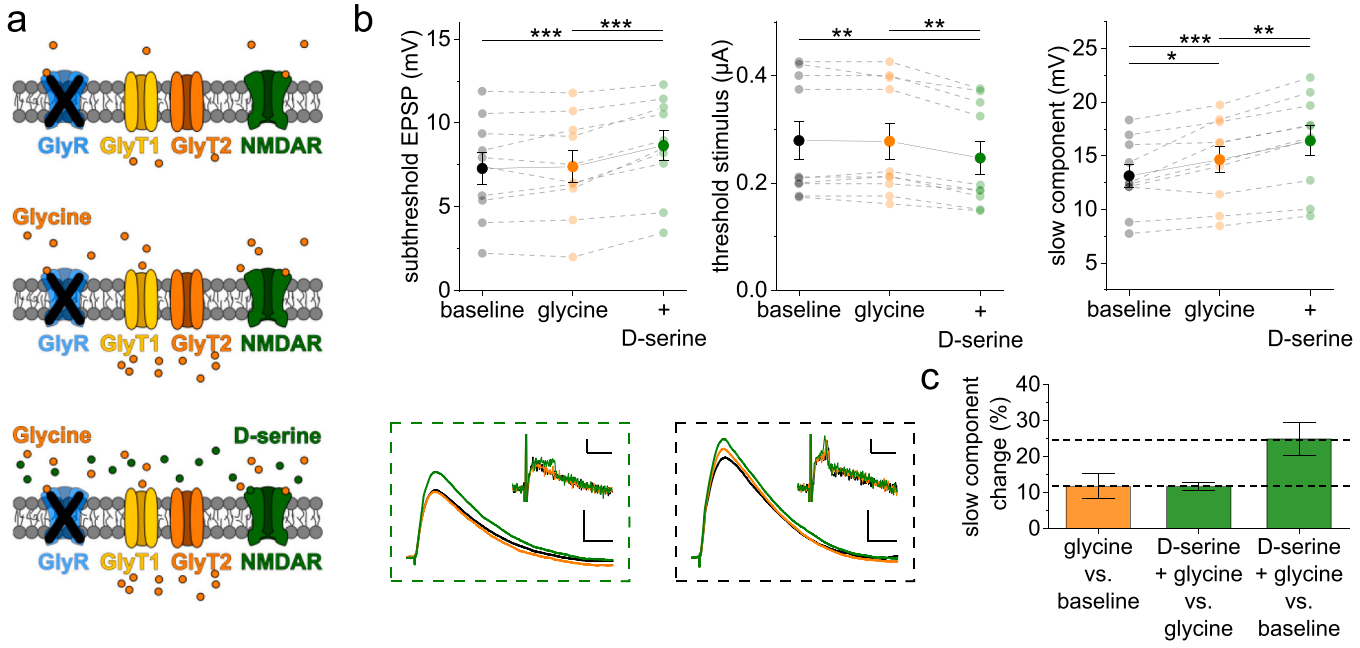

Fig. 2. Distinct effect of glycine and D-serine on dendritic spiking with intact glycine transport. a) Schematic of experimental protocol (GlyR inhibited, GlyT1 and GlyT2 not inhibited). Upper panel: baseline. Middle panel: bath application of 100 μM glycine (orange dots). Bottom panel: bath application of glycine and D-serine (10 μM). **b)** Glycine application does not change the subthreshold EPSP amplitude (left panel: 7.28 ± 0.94 mV vs. 7.39 ± 0.95 mV vs. 8.65 ± 0.91 mV, n = 10, F(2) = 20.07, p < 0.0001, one-way repeated measures ANOVA; post-hoc Tukey test, baseline vs. glycine q(18) = 0.64, p = 0.89) while additional application of D-serine does (baseline vs. D-serine q(18) = 8.06, p < 0.0001, glycine vs. D-serine q(18) = 7.42, p = 0.00015). The threshold stimulus is not changed by glycine, but adding D-serine decreased it (middle panel, 0.28 ± 0.03 μA vs. 0.28 ± 0.03 μA vs. 0.25 ± 0.03 μA, n = 10, $X^2(2) = 15.05$, p = 0.00054, Friedman ANOVA; post-hoc Dunn's test: baseline vs. glycine Z = 0.22, p = 1.00, baseline vs. D-serine Z = 3.47, p = 0.0016, glycine vs. D-serine Z = 3.24, p = 0.0036). The slow component amplitude is increased by glycine alone and further increased by adding D-serine (right panel, 13.13 ± 1.07 mV vs. 14.65 ± 1.22 mV vs. 16.40 ± 1.39 mV, n = 10, F(1.11) = 24.52, p = 0.00047, one-way repeated measures ANOVA; post-hoc Tukey test, baseline vs. glycine q(18) = 4.59, p = 0.012, baseline vs. D-serine q(18) = 9.90, p < 0.0001, glycine vs. D-serine q(18) = 5.30, p = 0.0040). Dashed boxes: sample traces of dendritic responses recorded during baseline (black), after application of glycine (orange) and after application of D-serine (green) at the threshold after D-serine application (left, green dashed boxed) and at the threshold during baseline and after glycine application (right, scale bars: 5 mV and 20 ms; inset: 1 mV/ms and 5 ms). **c)** Relative increases of slow component amplitudes from **b** reveals additive effects of D-serine and glycine under these conditions (glycine vs. baseline: orange, 12 ± 3.5 %; D-serine and glycine vs. glycine alone: green 12 ± 1.0 %; D-serine and glycine vs. baseline: green, 25 ± 4.5 %). Data are expressed and displayed as mean ± s.e.m.

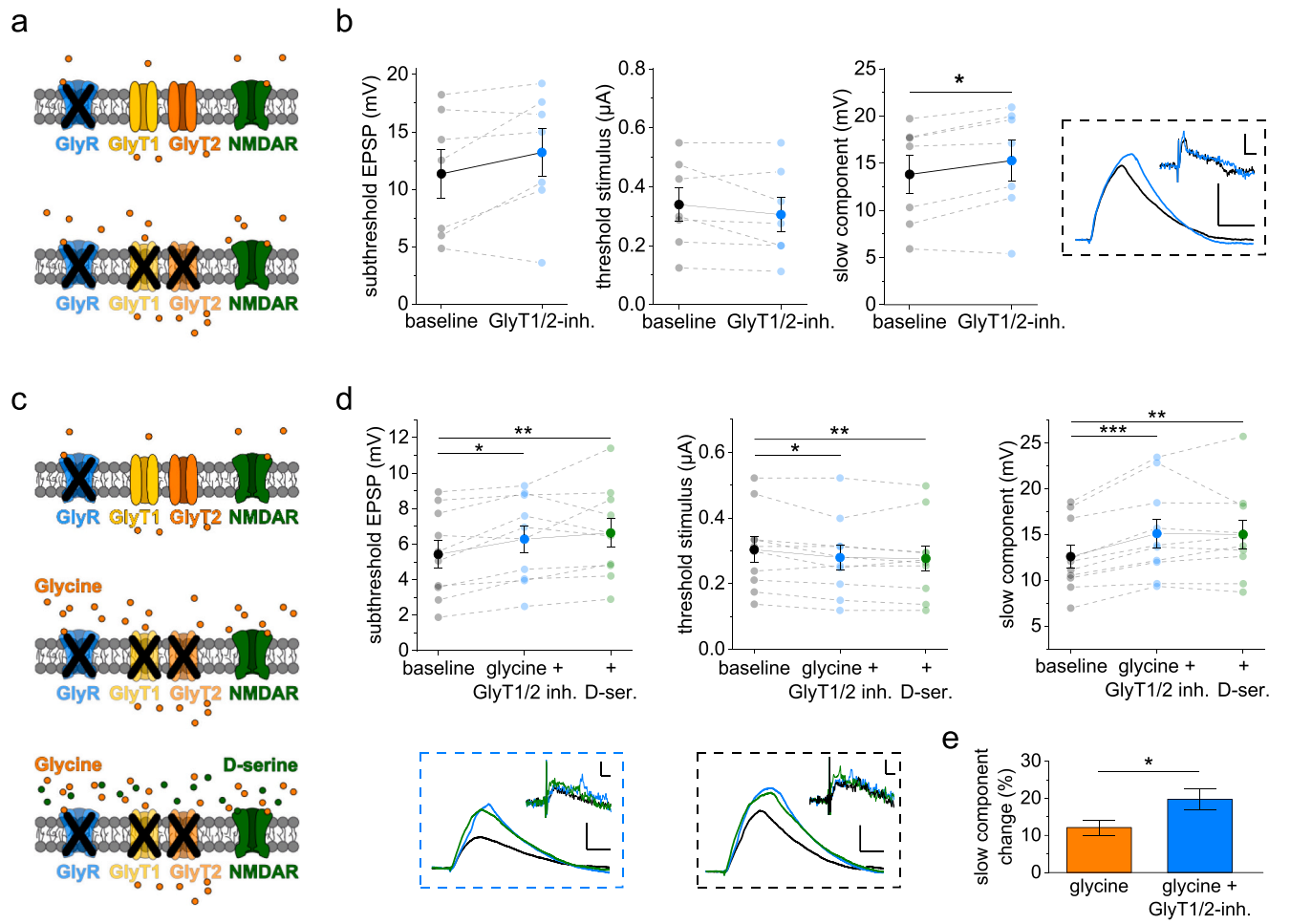

Fig. 3. Glycine transporters (GlyT1/2) control dendritic spiking and its responsiveness to glycine. a) Probing dendritic integration with GlyRs inhibited (upper panel, baseline) and its response to GlyT1/2 inhibition (lower panel, GlyT1/2-inh.) **b)** GlyT1/2 inhibition does not change subthreshold EPSPs (left panel, 11.34 ± 2.09 mV vs. 13.20 ± 2.07 mV, n = 7, t(6) = -1.97, p = 0.10, two-sided paired Student's t test) or the threshold stimulus of dendritic spikes (middle panel, 0.34 ± 0.057 µA vs. 0.31 ± 0.058 µA, n = 7, t(6) = 1.61, p = 0.16, two-sided paired Student's t test) but increases their slow component (right panel, 13.81 ± 2.05 mV vs. 15.27 ± 2.17 mV, n = 7, t(6) = -3.25, p = 0.017, two-sided paired Student's t test). Dashed box: example traces of dendritic spikes recorded during baseline (black) and after application of glycine transporter inhibitor (blue, scale bars: 5 mV and 20 ms, inset: 1 mV/ms and 5 ms). **c)** Probing dendritic integration with GlyRs inhibited (upper panel, baseline) and its response to combined GlyT1/2 inhibition and glycine application (middle panel, glycine + GlyT1/2-inh.) and combining this with D-serine application (lower panel, + D-ser.). **d)** Combining glycine application with GlyT1/2 inhibition increases subthreshold EPSP amplitudes (left panel, 5.42 ± 0.78 mV vs. 6.28 ± 0.76 mV vs. 6.63 ± 0.81 mV, n = 10, F(2) = 9.80, p = 0.0013, one-way repeated measures ANOVA; post-hoc Tukey test, baseline vs. glycine q(18) = 4.33, p = 0.018) which are not further increased by D-serine (baseline vs. D-serine q(18) = 6.08, p = 0.0012, glycine vs. D-serine q(18) = 1.75, p = 0.45). Similarly, the threshold stimulus is decreased (middle panel, 0.30 ± 0.039 µA vs. 0.28 ± 0.037 µA vs. 0.28 ± 0.038 µA, n = 10, F(2) = 7.28, p = 0.0048, one-way repeated measures ANOVA; post-hoc Tukey test: baseline vs. glycine q(18) = 4.37, p = 0.016, baseline vs. D-serine q(18) = 4.92, p = 0.0072, glycine vs. D-serine q(18) = 0.55, p = 0.92) and the slow component of dendritic spikes increased (right panel, 12.59 ± 1.24 mV vs. 15.10 ± 1.59 mV vs. 15.01 ± 1.55 mV, n = 10, F(2) = 12.86, p = 0.00034, one-way repeated measures ANOVA; post-hoc Tukey test, baseline vs. glycine q(18) = 6.32, p = 0.00083, baseline vs. D-serine q(18) = 6.10, p = 0.0012, glycine vs. D-serine q(18) = 0.22, p = 0.99) by glycine and GlyT1/2 inhibition without further changes by adding D-serine. Dashed boxes: sample traces of dendritic spikes recorded during baseline (black), after application of glycine together with GlyT1/2 inhibitors (blue) and after adding D-serine (green, scale bars: 5 mV and 20 ms, inset: 0.5 mV/ms and 5 ms) for the dendritic spike threshold during glycine application with GlyT1/2 inhibition (left, blue dashed box) and baseline (right, black dashed box). **e)** The relative change of the slow component amplitude for glycine application without GlyT1/2 inhibition (data from Fig. 1**e**) is significantly smaller than the change observed with GlyT1/2 inhibition **(d)** (12 ± 2.1 % vs. 20 ± 2.9 %, n = 23 and 10, t(31) = -2.09, p = 0.045, two-sided Student's t test). Data are expressed and displayed as mean ± s.e.m.

hippocampus is certain, the role of GlyT2 has been a matter of discussion (Xu and Gong, 2010). Therefore, the effects observed in Fig. 3 could result solely from GlyT1-dependent glycine uptake. To determine the contribution of GlyT1 alone to the control of dendritic spiking, we examined the effect of glycine applied together with the glycine transporter 1 (GlyT1) antagonists NFPS (5 µM) and then further added D-serine (as illustrated in Fig. 4**a**). Under these conditions, glycine led only to a small and insignificant increase of the subthreshold EPSP whereas further adding D-serine increased it compared to baseline (Fig. 4**b**, left panel), although there was no significant difference between the subthreshold EPSPs in glycine and added D-serine. The slow spike component was increased by glycine and GlyT1 inhibition and D-serine had an additional effect (Fig. 4**b** right panel), although a direct comparison of the slow component increases between glycine with GlyT1 inhibition and with GlyT1/2-inhibition (from Fig. 3) did only reveal a trend (Fig. 4**c**). Overall, the effects of additional D-serine when glycine was applied with a GlyT1-inhibitor alone suggest that GlyT2 can control extracellular glycine levels (see Fig. 3 for a comparison). The dendritic spike threshold stimulus was decreased by glycine combined with GlyT1 inhibition and added D-serine had no further effect (Fig. 4**b**, middle panel). This indicates that inhibition of GlyT1 alone is sufficient to enable a glycinergic modulation of the dendritic spike threshold (for

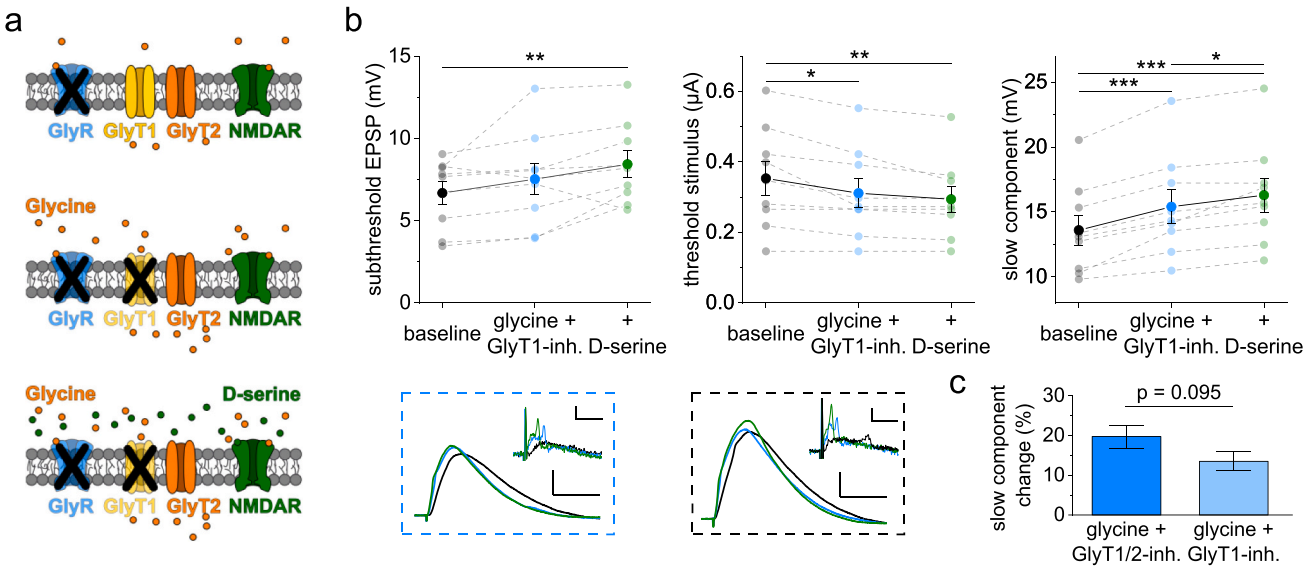

Fig. 4. Glycine transporter 1 (GlyT1) controls dendritic spiking and its responsiveness to glycine. a) Testing changes of dendritic integration with GlyRs inhibited (upper panel, baseline) induced by glycine application combined with GlyT1 inhibition (middle panel, glycine + GlyT1-inh.) and combining this with D-serine application (lower panel, + D-serine). **b)** Combining glycine application with only GlyT1 inhibition does not influence subthreshold EPSP amplitudes (left panel, 6.68 ± 0.69 mV vs. 7.52 ± 0.95 mV vs. 8.43 ± 0.83 mV, n = 9, F(2) = 5.73, p = 0.013, one-way repeated measures ANOVA; post-hoc Tukey test, baseline vs. glycine q(16) = 2.31, p = 0.26), but can be increased by D-serine (baseline vs. D-serine b vs. s q(16) = 4.79, p = 0.010, glycine vs. D-serine q(16) = 2.48, p = 0.22). Contrarily, the threshold stimulus is decreased (middle panel, 0.35 ± 0.05 vs. 0.31 ± 0.04 vs. 0.29 ± 0.04 µA, n = 9, F(2) = 10.33, p = 0.0013, one-way repeated measures ANOVA; post-hoc Tukey test: baseline vs. glycine q(16) = 4.42, p = 0.017, baseline vs. D-serine q(16) = 6.25, p = 0.0012, glycine vs. D-serine q(16) = 1.83, p = 0.42) by glycine and GlyT1 inhibition without further changes by adding D-serine. The slow component of dendritic spikes increased (right panel, 13.59 ± 1.15 mV vs. 15.40 ± 1.30 mV vs. 16.30 ± 1.30 mV, n = 9, F(2) = 43.26, p < 0.0001, one-way repeated measures ANOVA; post-hoc Tukey test, baseline vs. glycine q(16) = 8.63, p < 0.0001) by glycine and GlyT1 inhibition further increased by adding D-serine (baseline vs. D-serine q(16) = 12.91, p < 0.0001, glycine vs. D-serine q(16) = 4.23, p = 0.021). Dashed boxes: sample traces of dendritic spikes recorded during baseline (black), after application of glycine together with GlyT1 inhibitor (blue) and after adding D-serine (green, scale bars: 5 mV and 20 ms, inset: 2 mV/ms and 5 ms) for the dendritic spike threshold during glycine application with GlyT1 inhibition (left, blue dashed box) and baseline (right, black dashed box). **c)** Relative change of the slow component for glycine application with GlyT1/2 inhibition (data from Fig. 3**d**) is slightly, but not significantly, larger than the change observed with only GlyT1 inhibition **(b)** (20 ± 2.0 % vs. 14 ± 2.0 %, n = 10, and 9, Z = 1.67, p = 0.095, two-sided Mann-Whitney Test). Data are expressed and displayed as mean ± s.e.m.

comparison see Fig. 1).

2.2. *Glycine receptors can control the slow dendritic spike component*

Next, we investigated the role of glycine receptors (GlyRs) and tested if the effects of glycine and GlyT1/2 are different when the GlyR inhibitor strychnine is not present (Fig. 5). In previous experiments (Figs. 1–3**)** we included picrotoxin in the bath solution to isolate effects through glutamate receptor activation. However, picrotoxin was shown to partially inhibit GlyR-mediated currents (Chattipakorn and McMahon, 2002). We therefore replaced picrotoxin with the $GABA_A$ and $GABA_C$ inhibitors gabazine and TPMPA, respectively, to isolate effects mediated by glutamate and glycine receptors. We found that exogenous glycine on its own had no effect on dendritic excitability and spiking under these conditions (Fig. 5**a-b**), which indicates that inhibitory GlyRs counteract the effect of glycine on the slow spike component (Fig. 5**c**) when GlyT1/2 are functional. In contrast, glycine application combined with GlyT1/2 inhibition decreased the threshold stimulus and increased the slow component of the dendritic spike and the subthreshold EPSPs (Fig. 5**d-e**). This indicates that the inhibitory effect of GlyRs on the slow spike component can be overridden by increased glycine levels. Interestingly, this scenario of increased extracellular glycine, intact GlyRs and inhibited glycine uptake could correspond to the situation during activity-dependent endogenous glycine release (see Discussion) (Zhang et al., 2018), which illustrates that endogenous glycine release too could increase dendritic spiking. Identical experiments with picrotoxin instead of gabazine and TPMPA had qualitatively identical results (Supplementary Fig. 1).

Finally, we also analyzed subthreshold EPSPs throughout all experiments. First, we investigated those evoked by iontophoretic glutamate application with the highest stimulus intensity not inducing a dendritic spike (Fig. 1**c**, green dot and green trace). Throughout all experiments, changes of NMDAR co-agonist levels that affected the stimulus threshold had the opposite effect on these subthreshold EPSPs (e.g. glycine combined with GlyT1/2 inhibition decreasing the stimulus threshold and increasing the subthreshold EPSPs), except for the experiments, where only GlyT1 was blocked. This is consistent with the presence of an NMDAR-mediated component of the subthreshold EPSPs and cooperative action of NMDARs and dendritic voltage-dependent sodium in triggering dendritic spikes in CA1 pyramidal cells (Ariav et al., 2003; Losonczy and Magee, 2006; Bohmbach et al., 2022). Second, we examined evoked subthreshold EPSPs with an amplitude comparable to spontaneous EPSPs of ~ 1–2 mV (spontaneous-like EPSPs, sl-EPSPSs). None of the experimental conditions affected the amplitude of these (Supplementary table 2), which also implies that our experimental protocols did not induce synaptic plasticity.

3. Discussion

We analysed if and how extracellular glycine controls dendritic excitability and spiking of CA1 pyramidal cells, how its effect is shaped by glycine transporters (GlyT) and what roles two of its targets play (i.e., the NMDAR co-agonist binding site and inhibitory glycine receptors, GlyRs). Overall, we found that glycine is a potent regulator of dendritic spiking. It can decrease the amount of excitatory input needed for the generation of dendritic spikes and can increase their amplitude, thereby likely affecting the postsynaptic detection of simultaneous synaptic input and synaptic plasticity.

Between the two investigated targets of glycine, GlyRs play the less prominent role in controlling dendritic excitability and spiking. GlyRs

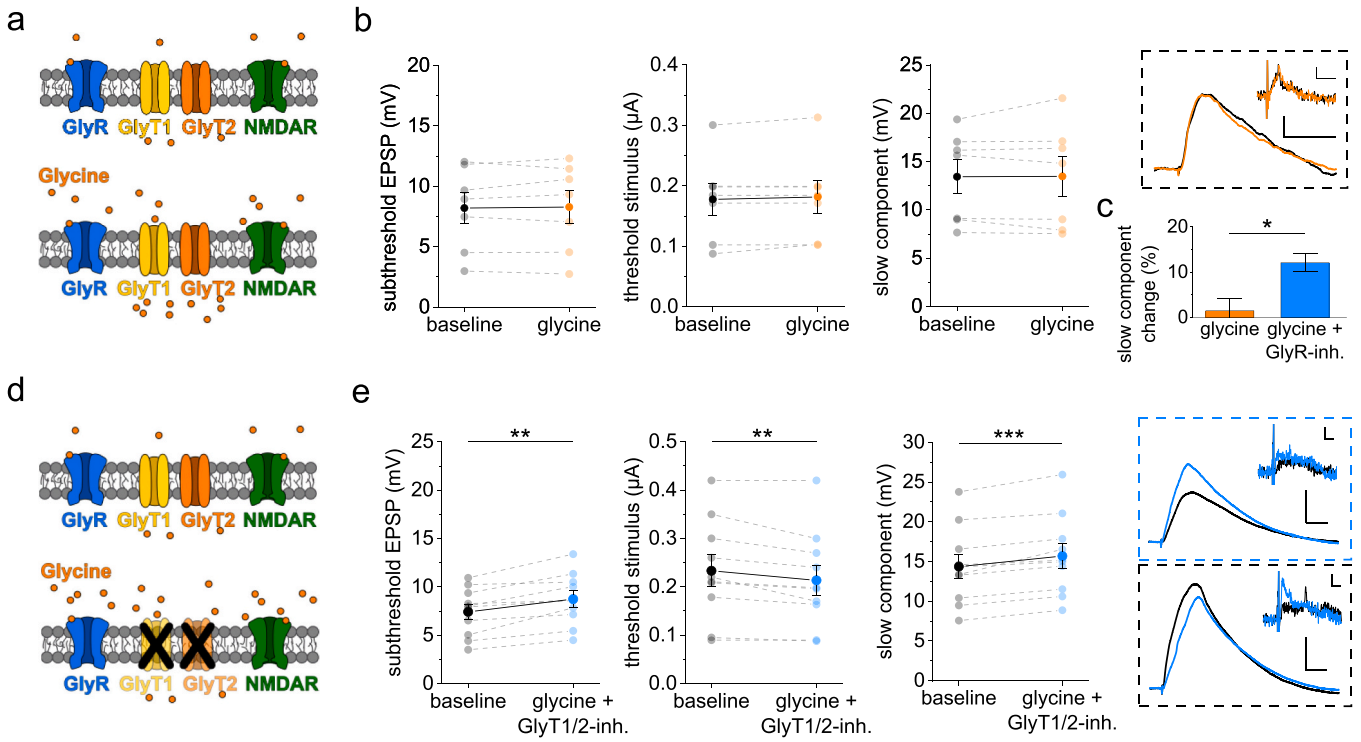

Fig. 5. Unblocking of inhibitory glycine receptors has a limited effect on the glycinergic control of dendritic spiking. a) Experimental protocol for **b**. Top panel: baseline, no GlyT1/2 or GlyR inhibitors. Bottom panel: acute bath application of glycine (orange dots). **b)** Under these conditions, glycine does not change subthreshold EPSP amplitudes (left panel, 8.20 ± 1.31 mV vs. 8.29 ± 1.37 mV, n = 7, t(6) = -0.41, p = 0.70, two-sided paired Student's t test), the threshold stimulus (middle panel, 0.18 ± 0.03 µA vs. 0.18 ± 0.03 µA, n = 7, t(6) = -1.52, p = 0.18, two-sided paired Student's t test) or the slow component of dendritic spikes (right panel, 13.44 ± 1.78 mV vs. 13.48 ± 2.04 mV, n = 7, t(6) = -0.10, p = 0.92, two-sided paired Student's t test). Dashed box: sample traces of dendritic spikes recorded during baseline (black) and after application of glycine (orange, scale bars: 2 mV and 20 ms, inset: 1 mV/ms and 5 ms). **c)** Relative change of the slow component for glycine application without GlyR blockade **(b)** is significantly smaller than the change observed with GlyRs blocked (data from Fig. 1**e**) (1.5 ± 2.8 % vs. 12 ± 2.1 %, n = 7 and 23, t(28) = -2.62, p = 0.014, two-sided Student's t test). **d)** Experimental protocol for **e**. Top panel: baseline, no GlyT1/2 or GlyR inhibitors. Bottom panel: acute bath application of glycine and GlyT1/2 inhibitors (GlyT1/2-inh.) **e)** With intact GlyRs, glycine and GlyT1/2 inhibition increased subthreshold EPSP amplitudes (left panel, 7.42 ± 0.79 mV vs. 8.74 ± 0.85 mV, n = 10, t(9) = -4.53, p = 0.0014, two-sided paired Student's t test), decreased the spike threshold (middle panel, 0.23 ± 0.03 µA vs. 0.21 ± 0.03 µA, n = 10, t(9) = 3.45, p = 0.0073, two-sided paired Student's t test) and increased their slow component (right panel, 14.35 ± 1.55 mV vs. 15.69 ± 1.60 mV, n = 10, t(9) = -5.39, p = 0.00044, two-sided paired Student's t test). Dashed boxes: sample traces of dendritic spikes recorded during baseline (black) and after application of glycine combined with GlyT1/2 inhibitors (blue, scale bars: 5 mV and 20 ms, inset: 0.5 mV/ms and 5 ms) at the threshold stimulus after application (top, blue dashed box) and during baseline (bottom, black dashed box). Data are expressed and displayed as mean ± s.e.m.

are well known to be expressed by hippocampal neurons (Xu and Gong, 2010) and can mediate a tonic inhibition especially when type I GlyTs are inhibited (Sipila et al., 2004; Zhang et al., 2008a). GlyRs can also control the direction of glycine-induced forms of synaptic long-term plasticity in the hippocampus (Chen et al., 2011; Zhang et al., 2014). Our experiments add a role of GlyRs in dampening the amplitude of the slow dendritic spike component under specific conditions. We observed that exogenous glycine increased this component when GlyRs were blocked (Fig. 1**e**) but not when GlyRs were available (Fig. 5**b** and **c**), which is in line with an GlyR-mediated inhibition of CA1 pyramidal cells when glycine levels are elevated (Sipila et al., 2004; Zhang et al., 2008a; Keck et al., 2008).

In contrast, glycine strongly promoted dendritic spiking via the NMDAR co-agonist binding site. The main evidence for this conclusion is that glycine occluded further effects of D-serine, the other NMDAR co-agonist with no other relevant known site of action, (Fig. 3**d**) and that the cumulative effect of glycine and D-serine does not exceed that of D-serine alone (see Fig. 2**c** and accompanying text). These results imply that exogenous D-serine and glycine increase dendritic spiking by acting on the co-agonist binding site of the same population of NMDARs in our experimental setting. Recently, the functional importance of so-called excitatory glycine receptors (eGlyRs), which are NMDARs composed of GluN3A and GluN1 subunits and are activated by glycine alone, has been demonstrated for cortical, amygdalar and hippocampal circuits (Bossi et al., 2022; Hurley et al., 2024; Pizzamiglio et al., 2025). However, because glycine directly activates eGlyRs whereas D-serine inhibits eGlyR-mediated currents (Chatterton et al., 2002; Bossi et al., 2022), eGlyRs are unlikely to contribute to the observed changes of dendritic spiking in our experiments, in which glycine and D-serine both increased dendritic spiking.

We also tested the role of GlyTs in controlling glycine effects on dendritic spiking, because it is well known that glycine transporters represent powerful uptake mechanisms that can efficiently lower extracellular glycine and counteract application of extracellular glycine (Berger et al., 1998; Bergeron et al., 1998; Chen et al., 2003; Sipila et al., 2004; Martina et al., 2004; Zhang et al., 2018; Supplisson, 2024). Our experiments with GlyT1/2 inhibition confirm that they can reduce the effect of exogenous glycine on NMDARs and, through that, strongly limit its effect on the dendritic response to excitatory input (compare Fig. 5**e** and Fig. 1**e**). Comparing effects of combining glycine application with GlyT1/2 inhibition and glycine application with only GlyT1 inhibition (Fig. 3**d** and Fig. 4) reveals a role of GlyT2 in controlling extracellular glycine levels. Although the role of GlyT2 in the hippocampus has been a matter of discussion (Xu and Gong, 2010), our findings are in line with immunohistochemical evidence for hippocampal GlyT2 expression (Danglot et al., 2004; Song et al., 2006). They are also consistent with our previous work using optical glycine sensors, which revealed a role of GlyT2 in controlling extracellular resting levels of glycine (Zhang et al.,

2018).

The involvement of GlyTs also has an interesting implication. The current view is that there are few, if any, glycinergic synapses in the hippocampus (Xu and Gong, 2010), which implies that extracellular glycine concentrations are primarily controlled by glycine transporters. Indeed, we have previously demonstrated that optically-detected activity-dependent glycine release is inhibited by GlyT1/2 inhibition in the hippocampus (Zhang et al., 2018). Further experiments revealed that resting levels of extracellular glycine are kept low by each of the two transporters, GlyT1 and 2, as well. Thus, GlyT1/2 reduce the extracellular glycine during periods of low neuronal/cellular activity but reverse to release glycine into the extracellular space when neuronal activity is high (Zhang et al., 2018), which is compatible with the stoichiometry and properties of GlyT1-mediated glycine transport (Roux and Supplisson, 2000). The conditions under which activity-dependent glycine release occurs (reverse transport and therefore impaired uptake) are qualitatively similar to experimental GlyT1/2 inhibition combined with glycine application (Fig. 5**e**). For these reasons, we predict that activity-dependent endogenous glycine release increases the dendritic response to excitatory input and dendritic spiking similar to Fig. 5**e**.

Testing this hypothesis may not be straightforward. GlyT1 is the transporter that most likely reverses because of its stoichiometry (Roux and Supplisson, 2000). It is expressed by astrocytes and also pre- and postsynaptically at glutamatergic synapses (Cubelos et al., 2005; Xu and Gong, 2010), which complicates an experimental analysis because all three compartment could potentially take up and/or release glycine. Similarly, it is not possible to conclude from our present experiments, which GlyT-expressing cell types and compartments (e.g. perisynaptic astrocytic processes, pre- and postsynaptic sites) play specific role in controlling glycinergic modulation of dendritic integration and dendritic spiking. Also, we do not experimentally distinguish populations of NMDAR with different subunits composition (e.g. GluN2A vs. GluN2B containing NMDARs) precluding insights into their selective regulation by glycine (Papouin et al., 2012). Glycine was also shown to induce internalization of surface NMDARs and to affect their trafficking (Nong et al., 2003; Ferreira et al., 2017). Especially, rapid internalization of NMDARs after glycine applications could affect our experimental results and their interpretation. The concentration-dependence of glycine-induced NMDAR internalisation varies widely between individual reports (Nong et al., 2003; Martina et al., 2004; Zhang et al., 2008b; Chen et al., 2011; Cappelli et al., 2022), and we have chosen a concentration of 100 μM because two reports indicate that this concentration reliably increases NDMAR-mediated synaptic currents without inducing internalisation in acute slices (Chen et al., 2003; Cappelli et al., 2022). Even if glycine-induced internalisation is present in our experiments, it would lead to an underestimation of how strongly glycine facilitates dendritic spiking.

Overall, our experiments reveal a significant impact of glycine and its transporters on the dendritic integration of excitatory synaptic input and the generation of dendritic spikes in CA1 pyramidal cells. This is likely to play a role in situations, in which activity-dependent glycine release occurs such as plasticity-inducing activity (Zhang et al., 2018) (see above) or pathophysiological activity like in epilepsy (Ronne-Engström et al., 1992). These are therefore predicted to lead to increased dendritic spiking and may thereby modify for instance hippocampal place coding and memory formation (Bohmbach et al., 2022; Masala et al., 2023). However, it remains to be tested if dendritic integration of clustered synaptic input in a physiological setting (e.g. in vivo) displays the same dependency on glycine and glycine transport as observed here. Nonetheless, our findings could be important regarding the therapeutic use of GlyTs to counteract NMDAR hypofunction in diseases like schizophrenia (Möhler et al., 2011; Nakazawa and Sapkota, 2020). Our results imply that interpreting the clinical effects of GlyT inhibitors (Lane et al., 2010; Fleischhacker et al., 2021; Rosenbrock et al., 2023) needs to consider a potentially wide-spread effect on dendritic integration and spiking.

3.1. STAR methods

Key resources table

Key resources tableREAGENT or RESOURCE	SOURCE	IDENTIFIER
Chemicals, peptides, and recombinant proteins		
Alexa Fluor 594 Hydrazide	ThermoFisher	A10438
D-serine	Sigma	S4250
Fluo-4, Pentapotassium Salt	ThermoFisher	F14200
Gabazine	Tocris	1262
Glutamic acid (L-)	AppliChem	A3723
Glycine	AppliChem	A1067
NFPS	Tocris	2789
Org 25543	Tocris	4782
Picrotoxin	abcam	Asc-315
Strychnine hydrochloride	Sigma	S8753
TPMPA	Tocris	1040
Experimental models: Organisms/strains		
Wistar rats	Charles River	Strain Code 003
Software and algorithms		
Origin Pro 2017 and 2024	OriginLab	https://www.originlab.com/
pClamp 10.3	Molecular Devices	https://www.moleculardevices.com/

3.2. Experimental model and subject details

All research and experimental procedures complied with the relevant ethical regulations. All animal procedures were conducted in accordance with the regulations of the European Commission and all relevant national and institutional guidelines and requirements (e.g. Haus für Experimentelle Therapie [HET], University Hospital Bonn, Germany). All animals used in this study were housed under 12 h light/dark conditions and were allowed ad libitum access to food and water (room temperature 22 °C, air humidity 50–70 %). All experiments were performed on 3–5-week-old male Wistar rats in the CA1 region of the hippocampus.

4. Method details

4.1. Hippocampal slice preparation

Acute brain slices were prepared as described previously (Bohmbach et al., 2022). Briefly, after deeply anesthetizing the animals with isoflurane, it was decapitated and the brain quickly removed from the skull. Horizontal hippocampal slices, 300 μm thick, were prepared in an ice-cold slicing solution (in mM: sucrose 105, NaCl 60, KCl 2.5, MgCl2 7, NaH2PO4 1.25, ascorbic acid 1.3, sodium pyruvate 3, NaHCO3 26, CaCl2 0.5 and glucose 10; osmolarity 300–310 mOsm/l). Slices were kept for 15 min in slicing solution at 34°C before transferring them to artificial cerebrospinal fluid (ACSF, composition in mM: NaCl 131, KCl 2.5, MgSO4 1.3, NaH2PO4 1.25, NaHCO3 21, CaCl2 2 and glucose 10; pH 7.35–7.45; osmolarity 297–303 mOsm/l). Slices were allowed to rest at least 1 h at RT before the experiments. All experiments were conducted at ~ 34 °C.

4.2. Glutamate iontophoresis

Glutamate iontophoresis experiments were performed as previously described (Bohmbach et al., 2022). Briefly, acute slices were transferred to a submersion-type recording chamber mounted on a Scientifica 2PE fluorescence microscope with a 40x/0.8 NA objective (Olympus) and superfused with ACSF at 34°C containing 50 μM picrotoxin and where indicated strychnine hydrochloride 0.5 μM. For the experiments shown in Figs. 4, 5 μM gabazine and 50 μM TPMPA were used instead of picrotoxin. CA1 pyramidal cells were patched in the whole-cell configuration (using a Multiclamp 700B amplifier) with borosilicate glass

pipettes (3–5 MΩ resistance, GB150F-10, Science Products) filled with an intracellular solution containing (in mM): KCH_3O_3S 135, HEPES 10, di-Tris-Phosphocreatine 10, $MgCl_2$ 4, Na_2-ATP 4, Na-GTP 0.4, Alexa Fluor 594 hydrazide 0.04, Fluo-4 pentapotassium salt 0.2, pH adjusted to 7.2 using KOH, osmolarity 290–295 mOsm/l. Cells were kept in the current clamp mode. Local dendritic glutamate applications were performed with a microiontophoresis system (MVCS-C-01C-150, NPI) and borosilicate glass pipettes (60–90 MΩ resistance, GB150F-10, Science Products), filled with 150 mM glutamic acid (pH adjusted to 7.0 with NaOH) and 50 μM Alexa Fluor 594 hydrazide. Under guidance of two-photon excitation fluorescence microscopy (Ti:sapphire pulsed laser, Vision S, Coherent, excitation at $\lambda = 800$ nm), the microiontophoresis pipette was placed in close proximity (<1 μm) to a spine on an apical oblique dendrite in the *stratum radiatum* (typically 40–80 μm below the slice surface). Only cells with an initial access resistance (R_a) < 20 MΩ and with < 20 % change during the time course of the recording were included in the analysis. The iontophoretic stimulation duration was adjusted (duration < 0.8 ms) so that reliable somatic excitatory postsynaptic potentials (EPSPs), dendritic spikes and somatic action potentials could be recorded with increasing stimulation intensity (10–50 pA steps until the occurrence of an AP, 3 s interstimulus interval). See beginning of results section, Fig. 1 and (Bohmbach et al., 2022) for details on the analysis of postsynaptic responses and dendritic spiking.

4.3. Pharmacology

The following drugs in the respective concentrations were used: 10 μM D-serine, 100 μM glycine, 5 μM gabazine, 5 μM NFPS (inhibitor of GlyT1), 1 μM Org 25543 (inhibitor of GlyT2), 50 μM picrotoxin, 0.5 μM strychnine hydrochloride, 50 μM TPMPA. Recordings were performed 5–8 min after the bath application of the drug in the sequences illustrated in the figure.

4.4. Quantification and statistical analysis

Data and statistical analyses were done with pClamp 10.3 (Molecular Devices) and OriginPro 2017 or 2024 (OriginLab). Statistical tests were performed after investigating whether data followed a normal distribution (Shapiro-Wilk test). Depending on the outcome, statistical tests were performed using non-parametric (Friedman test, Wilcoxon signed-rank test) or parametric (repeated measures ANOVA, Student's *t*-tests) approaches as indicated. All tests are two-sided. Data are expressed and displayed as mean ± s.e.m. (standard error of mean). In graphs, asterisks indicate statistical significance. * for $p < 0.05$, ** for $p < 0.01$ and *** for $p < 0.001$.

CRediT authorship contribution statement

Bauer Vincent: Writing – review & editing, Visualization, Data curation. **Kirsten Bohmbach:** Writing – review & editing, Visualization, Data curation. **Christian Henneberger:** Writing – review & editing, Writing – original draft, Visualization, Supervision, Funding acquisition, Conceptualization.

Declaration of Competing Interest

The authors declare that they have no known competing financial interests or personal relationships that could have appeared to influence the work reported in this paper.

Acknowledgements

We thank Thomas Erdmann and Erik Sommer for administrative and technical support. Research was supported by the German Research Foundation (DFG; SFB1089 B03 to C.H.).

Author contributions

K.B. and V.B. performed and analyzed all experiments. C.H. conceived the research project and wrote the initial version of the manuscript, to which then all authors contributed.

Data and code availability

The data supporting the current study have not been deposited in a public repository but are available upon reasonable request from the lead contact.

Appendix A. Supporting information

Supplementary data associated with this article can be found in the online version at doi:10.1016/j.pneurobio.2025.102856.

References

Adamsky, A., Kol, A., Kreisel, T., Doron, A., Ozeri-Engelhard, N., Melcer, T., Refaeli, R., Horn, H., Regev, L., Groysman, M., London, M., Goshen, I., 2018. Astrocytic activation generates de novo neuronal potentiation and memory enhancement. Cell 174, 59–71.

Ariav, G., Polsky, A., Schiller, J., 2003. Submillisecond precision of the input-output transformation function mediated by fast sodium dendritic spikes in basal dendrites of CA1 pyramidal neurons. J. Neurosci. 23, 7750–7758.

Berger, A.J., Dieudonné, S., Ascher, P., 1998. Glycine uptake governs glycine site occupancy at NMDA receptors of excitatory synapses. J. Neurophysiol. 80, 3336–3340.

Bergeron, R., Meyer, T.M., Coyle, J.T., Greene, R.W., 1998. Modulation of N-methyl-D-aspartate receptor function by glycine transport. Proc. Natl. Acad. Sci. USA 95, 15730–15734.

Bohmbach, K., Masala, N., Schönhense, E.M., Hill, K., Haubrich, A.N., Zimmer, A., Opitz, T., Beck, H., Henneberger, C., 2022. An astrocytic signaling loop for frequency-dependent control of dendritic integration and spatial learning. Nat. Commun. 13, 7932.

Bossi, S., Dhanasobhon, D., Ellis-Davies, G.C.R., Frontera, J., de Brito Van Velze, M., Lourenço, J., Murillo, A., Luján, R., Casado, M., Perez-Otaño, I., Bacci, A., Popa, D., Paoletti, P., Rebola, N., 2022. GluN3A excitatory glycine receptors control adult cortical and amygdalar circuits. Neuron 110, 2438–2454.e8.

Bossi, S., Pizzamiglio, L., Paoletti, P., 2023. Excitatory GluN1/GluN3A glycine receptors (eGlyRs) in brain signaling. Trends Neurosci. 46, 667–681.

Cappelli, J., Khacho, P., Wang, B., Sokolovski, A., Bakkar, W., Raymond, S., Ahlskog, N., Pitney, J., Wu, J., Chudalayandi, P., Wong, A.Y.C., Bergeron, R., 2022. Glycine-induced NMDA receptor internalization provides neuroprotection and preserves vasculature following ischemic stroke. iScience 25, 103539.

Chatterton, J.E., Awobuluyi, M., Premkumar, L.S., Takahashi, H., Talantova, M., Shin, Y., Cui, J., Tu, S., Sevarino, K.A., Nakanishi, N., Tong, G., Lipton, S.A., Zhang, D., 2002. Excitatory glycine receptors containing the NR3 family of NMDA receptor subunits. Nature 415, 793–798.

Chattipakorn, S.C., McMahon, L.L., 2002. Pharmacological characterization of glycine-gated chloride currents recorded in rat hippocampal slices. J. Neurophysiol. 87, 1515–1525.

Chen, L., Muhlhauser, M., Yang, C.R., 2003. Glycine tranporter-1 blockade potentiates NMDA-mediated responses in rat prefrontal cortical neurons in vitro and in vivo. J. Neurophysiol. 89, 691–703.

Chen, P.E., Geballe, M.T., Katz, E., Erreger, K., Livesey, M.R., O'Toole, K.K., Le, P., Lee, C. J., Snyder, J.P., Traynelis, S.F., Wyllie, D.J.A., 2008. Modulation of glycine potency in rat recombinant NMDA receptors containing chimeric NR2A/2D subunits expressed in Xenopus laevis oocytes. J. Physiol. 586, 227–245.

Chen, R.-Q., Wang, S.-H., Yao, W., Wang, J.-J., Ji, F., Yan, J.-Z., Ren, S.-Q., Chen, Z., Liu, S.-Y., Lu, W., 2011. Role of glycine receptors in glycine-induced LTD in hippocampal CA1 pyramidal neurons. Neuropsychopharmacology 36, 1948–1958.

Cubelos, B., Giménez, C., Zafra, F., 2005. Localization of the GLYT1 glycine transporter at glutamatergic synapses in the rat brain. Cereb. Cortex 15, 448–459.

Danglot, L., Rostaing, P., Triller, A., Bessis, A., 2004. Morphologically identified glycinergic synapses in the hippocampus. Mol. Cell. Neurosci. 27, 394–403.

Ferreira, J.S., Papouin, T., Ladépêche, L., Yao, A., Langlais, V.C., Bouchet, D., Dulong, J., Mothet, J.-P., Sacchi, S., Pollegioni, L., Paoletti, P., Oliet, S.H.R., Groc, L., 2017. Co-agonists differentially tune GluN2B-NMDA receptor trafficking at hippocampal synapses. eLife 6, e25492.

Fleischhacker, W.W., Podhorna, J., Gröschl, M., Hake, S., Zhao, Y., Huang, S., Keefe, R.S. E., Desch, M., Brenner, R., Walling, D.P., Mantero-Atienza, E., Nakagome, K., Pollentier, S., 2021. Efficacy and safety of the novel glycine transporter inhibitor BI 425809 once daily in patients with schizophrenia: a double-blind, randomised, placebo-controlled phase 2 study. Lancet Psychiatry 8, 191–201.

Harnett, M.T., Makara, J.K., Spruston, N., Kath, W.L., Magee, J.C., 2012. Synaptic amplification by dendritic spines enhances input cooperativity. Nature 491, 599–602.

Henneberger, C., Papouin, T., Oliet, S.H.R., Rusakov, D.A., 2010. Long-term potentiation depends on release of D-serine from astrocytes. Nature 463, 232–236.
Hurley, E.P., Mukherjee, B., Fang, L.Z., Barnes, J.R., Barron, J.C., Nafar, F., Hirasawa, M., Parsons, M.P., 2024. GluN3A and excitatory glycine receptors in the adult hippocampus. J. Neurosci. https://doi.org/10.1523/JNEUROSCI.0401-24.2024.
Johnson, J.W., Ascher, P., 1987. Glycine potentiates the NMDA response in cultured mouse brain neurons. Nature 325, 529–531.
Keck, T., Lillis, K.P., Zhou, Y.-D., White, J.A., 2008. Frequency-dependent glycinergic inhibition modulates plasticity in hippocampus. J. Neurosci. 28, 7359–7369.
Kleckner, N.W., Dingledine, R., 1988. Requirement for glycine in activation of NMDA-receptors expressed in Xenopus oocytes. Science 241, 835–837.
Koh, W., et al., 2022. Astrocytes render memory flexible by releasing D-serine and regulating NMDA receptor tone in the hippocampus. Biol. Psychiatry 91, 740–752.
Lane, H.-Y., Lin, C.-H., Huang, Y.-J., Liao, C.-H., Chang, Y.-C., Tsai, G.E., 2010. A randomized, double-blind, placebo-controlled comparison study of sarcosine (N-methylglycine) and D-serine add-on treatment for schizophrenia. Int. J. Neuropsychopharmacol. 13, 451–460.
Losonczy, A., Magee, J.C., 2006. Integrative properties of radial oblique dendrites in hippocampal CA1 pyramidal neurons. Neuron 50, 291–307.
Lozovaya, N., Yatsenko, N., Beketov, A., Tsintsadze, T., Burnashev, N., 2005. Glycine receptors in CNS neurons as a target for nonretrograde action of cannabinoids. J. Neurosci. 25, 7499–7506.
Martina, M., Gorfinkel, Y., Halman, S., Lowe, J.A., Periyalwar, P., Schmidt, C.J., Bergeron, R., 2004. Glycine transporter type 1 blockade changes NMDA receptor-mediated responses and LTP in hippocampal CA1 pyramidal cells by altering extracellular glycine levels. J. Physiol. 557, 489–500.
Masala, N., Pofahl, M., Haubrich, A.N., Sameen Islam, K.U., Nikbakht, N., Pasdarnavab, M., Bohmbach, K., Araki, K., Kamali, F., Henneberger, C., Golcuk, K., Ewell, L.A., Blaess, S., Kelly, T., Beck, H., 2023. Targeting aberrant dendritic integration to treat cognitive comorbidities of epilepsy. Brain 146, 2399–2417.
Matsui, T., Sekiguchi, M., Hashimoto, A., Tomita, U., Nishikawa, T., Wada, K., 1995. Functional comparison of D-serine and glycine in rodents: the effect on cloned NMDA receptors and the extracellular concentration. J. Neurochem. 65, 454–458.
Möhler, H., Boison, D., Singer, P., Feldon, J., Pauly-Evers, M., Yee, B.K., 2011. Glycine transporter 1 as a potential therapeutic target for schizophrenia-related symptoms: evidence from genetically modified mouse models and pharmacological inhibition. Biochem. Pharmacol. 81, 1065–1077.
Nakazawa, K., Sapkota, K., 2020. The origin of NMDA receptor hypofunction in schizophrenia. Pharmacol. Ther. 205, 107426.
Nong, Y., Huang, Y.-Q., Ju, W., Kalia, L.V., Ahmadian, G., Wang, Y.T., Salter, M.W., 2003. Glycine binding primes NMDA receptor internalization. Nature 422, 302–307.
Papouin, T., Ladépêche, L., Ruel, J., Sacchi, S., Labasque, M., Hanini, M., Groc, L., Pollegioni, L., Mothet, J.-P., Oliet, S.H.R., 2012. Synaptic and Extrasynaptic NMDA Receptors Are Gated by Different Endogenous Coagonists. Cell 150, 633–646.
Papouin, T., Dunphy, J.M., Tolman, M., Dineley, K.T., Haydon, P.G., 2017. Septal cholinergic neuromodulation tunes the astrocyte-dependent gating of hippocampal NMDA receptors to wakefulness. Neuron 94, 840–854.
Pizzamiglio, L., Morice, E., Cardoso, C., Bossi, S., Mailhes-Hamon, C., Heimendahl, M. von, Girardeau, G., Paoletti, P., 2025. Excitatory glycine receptors control ventral hippocampus synaptic plasticity and anxiety-related behaviors. Proc. Natl. Acad. Sci. USA 122, e2501118122.
Poirazi, P., Papoutsi, A., 2020. Illuminating dendritic function with computational models. Nat. Rev. Neurosci. 21, 303–321.
Remy, S., Spruston, N., 2007. Dendritic spikes induce single-burst long-term potentiation. Proc. Natl. Acad. Sci. USA 104, 17192–17197.
Robin, L.M., et al., 2018. Astroglial CB1 receptors determine synaptic D-serine availability to enable recognition memory. Neuron 98, 935–944.
Ronne-Engström, E., Hillered, L., Flink, R., Spännare, B., Ungerstedt, U., Carlson, H., 1992. Intracerebral microdialysis of extracellular amino acids in the human epileptic focus. J. Cereb. Blood Flow. Metab. 12, 873–876.
Rosenbrock, H., Desch, M., Wunderlich, G., 2023. Development of the novel GlyT1 inhibitor, iclepertin (BI 425809), for the treatment of cognitive impairment associated with schizophrenia. Eur. Arch. Psychiatry Clin. Neurosci. 273, 1557–1566.
Roux, M.J., Supplisson, S., 2000. Neuronal and glial glycine transporters have different stoichiometries. Neuron 25, 373–383.
Sheffield, M.E.J., Adoff, M.D., Dombeck, D.A., 2017. Increased prevalence of calcium transients across the dendritic arbor during place field formation. Neuron 96, 490–504.e5.
Sipila, S., Huttu, K., Voipio, J., Kaila, K., 2004. GABA uptake via GABA transporter-1 modulates GABAergic transmission in the immature hippocampus. J. Neurosci. 24, 5877–5880.
Song, W., Chattipakorn, S.C., McMahon, L.L., 2006. Glycine-gated chloride channels depress synaptic transmission in rat hippocampus. J. Neurophysiol. 95, 2366–2379.
Stuart, G.J., Spruston, N., 2015. Dendritic integration: 60 years of progress. Nat. Neurosci. 18, 1713–1721.
Supplisson, S., 2024. Dynamic role of GlyT1 as glycine sink or source: Pharmacological implications for the gain control of NMDA receptors. Neuroscience. https://doi.org/10.1016/j.neuroscience.2024.07.037.
Tsai, G., Ralph-Williams, R.J., Martina, M., Bergeron, R., Berger-Sweeney, J., Dunham, K. S., Jiang, Z., Caine, S.B., Coyle, J.T., 2004. Gene knockout of glycine transporter 1: characterization of the behavioral phenotype. Proc. Natl. Acad. Sci. USA 101, 8485–8490.
Xu, T.-L., Gong, N., 2010. Glycine and glycine receptor signaling in hippocampal neurons: Diversity, function and regulation. Prog. Neurobiol. 91, 349–361.
Zhang, L.-H., Gong, N., Fei, D., Xu, L., Xu, T.-L., 2008a. Glycine Uptake Regulates Hippocampal Network Activity via Glycine Receptor-Mediated Tonic Inhibition. Neuropsychopharmacol 33, 701–711.
Zhang, W.H., Herde, M.K., Mitchell, J.A., Whitfield, J.H., Wulff, A.B., Vongsouthi, V., Sanchez-Romero, I., Gulakova, P.E., Minge, D., Breithausen, B., Schoch, S., Janovjak, H., Jackson, C.J., Henneberger, C., 2018. Monitoring hippocampal glycine with the computationally designed optical sensor GlyFS. Nat. Chem. Biol. 14, 861–869.
Zhang, X.-Y., Ji, F., Wang, N., Chen, L.-L., Tian, T., Lu, W., 2014. Glycine induces bidirectional modifications in N-Methyl-d-aspartate receptor-mediated synaptic responses in hippocampal CA1 neurons. J. Biol. Chem. 289, 31200–31211.
Zhang, Z., Gong, N., Wang, W., Xu, L., Xu, T.-L., 2008b. Bell-shaped D-serine actions on hippocampal long-term depression and spatial memory retrieval. Cereb. Cortex 18, 2391–2401.